CVD Synthetic Diamonds from Gemesis Corp.

Wuyi Wang, Ulrika F. S. D'Haenens-Johansson, Paul Johnson, Kyaw Soe Moe, Erica Emerson, Mark E. Newton, and Thomas M. Moses

Gemological and spectroscopic properties of CVD synthetic diamonds from Gemesis Corp. were examined. Their color (colorless, near-colorless, and faint, ranging from F to L) and clarity (typically VVS) grades were comparable to those of top natural diamonds, and their average weight was nearly 0.5 ct. Absorption spectra in the mid- and near-infrared regions were free from defect-related features, except for very weak absorption attributed to isolated nitrogen, but all samples were classified as type IIa. Varying intensities of $[Si\text{-}V]^-$ and isolated nitrogen were detected with UV-Vis-NIR absorption spectroscopy. Electron paramagnetic resonance was used to quantify the neutral single substitutional nitrogen content. Photoluminescence spectra were dominated by N-V centers, $[Si\text{-}V]^-$, H3, and many unassigned weak emissions. The combination of optical centers strongly suggests that post-growth treatments were applied to improve color and transparency. PL spectroscopy at low temperature and UV fluorescence imaging are critical in separating these synthetic products from their natural counterparts.

Along with the conventional high-pressure, high-temperature (HPHT) growth technique, single-crystal synthetic diamond can be produced using chemical vapor deposition (CVD). Technological advances and a greater understanding of the crystal growth processes have led to significant improvements in quality over the last decade. Today, CVD-grown faceted synthetic diamonds are present in the jewelry market in a variety of colors and sizes (e.g., Wang et al., 2003, 2005; Martineau et al., 2004). Furthermore, post-growth treatments to improve the color and transparency of these materials have been investigated.

In November 2010 Gemesis Corp., a well-known manufacturer of gem-quality HPHT synthetic diamonds, announced plans to market colorless and near-colorless CVD synthetics (Graff, 2010). Since March 2012, the company has sold mounted and loose CVD synthetic diamonds (e.g., figure 1).

Because of the high cost and difficulty to manufacture colorless HPHT synthetics, growth methods have traditionally focused on fancy colors. However, now it is colorless and near-colorless CVD synthetics, such as those developed by Gemesis, that pose the greatest commercial challenge to natural diamonds (treated and untreated) of comparable quality. This study follows an initial report by Wang and Moses (2011) and presents gemological characteristics and spectroscopic features of new CVD synthetics from Gemesis. Key identification features that help separate these products from natural diamonds are also discussed.

CVD Growth. While HPHT growth takes place under temperature and pressure conditions in which diamond is the stable phase of carbon, the CVD technique enables growth under conditions where diamond is metastable with respect to graphite. This means that although diamond is kinetically stable, it is thermodynamically unstable. The technique is based on a gas-phase chemical reaction involving a hydrocarbon gas (such as methane) in an excess of hydrogen gas occurring above a substrate. For single-crystal synthetic diamond growth the substrate is also a synthetic diamond, usually in the form of a {100}-oriented polished plate. Multiple substrates can be placed simultaneously in the CVD reaction chamber.

See end of article for About the Authors and Acknowledgments.
Gems & Gemology, Vol. 48, No. 2, pp. 80–97,
http://dx.doi.org/10.5741/GEMS.48.2.80.

Figure 1. These faceted CVD synthetic diamond samples (0.24–0.90 ct) obtained from Gemesis Corp. were examined in this study. Color grades are mainly in the range of colorless to near-colorless, and clarity is dominantly in VVS or better categories. These features are comparable to top-quality natural counterparts. Composite photo by Jian Xin (Jae) Liao.

The gas-phase precursor molecules can be activated in a variety of ways, typically by microwaves. Once the complex chain of reactions has been initiated, carbon atoms are added to the substrate (see Overview article on pp. 124–127 of this issue). The growth parameters are optimized to ensure the formation of a tetrahedrally bonded (sp^3) carbon lattice, of which diamond is composed, rather than sp^2-bonded graphitic material, and that the latter material is selectively etched. The reactions occur at pressures of 10–200 torr, and the substrate is held at temperatures ranging from 700 to 1,000°C during the active growth period.

One of the main advantages of the CVD method is the ability to dope the synthesized diamond by the controlled addition of gases containing the intended impurity atom (e.g., nitrogen, silicon, or boron). Nevertheless, unintentional impurity doping can also occur due to their presence in the gas sources or the reactor components. Goodwin and Butler (1997) and Butler et al. (2009) provided a thorough review of the important features of the synthesis environment and critical aspects of the growth process.

HPHT Processing for the Removal of Brown Color. Interest in the cause of brown color in both natural and CVD-grown type IIa diamond has heightened ever since it was reported that HPHT treatment could decolorize these goods and greatly improve their commercial value (Moses et al., 1999; Fisher and Spits, 2000; Wang et al., 2003; Martineau et al., 2004). The color arises from a gradual, featureless rise in the absorption spectrum from ~1200 nm to the diamond absorption edge at ~225 nm. No specific threshold for the rise has been identified, and it has been suggested that the absorption originates from extended defects rather than impurity-related point defects (Hounsome et al., 2006). Most brown CVD synthetics also show broad bands at 365 and 520 nm, and absorption from the latter band may further contribute to the color intensity (Martineau et al., 2004).

The brown color in natural diamond is often concentrated along slip bands (though not all plastically deformed diamonds are brown), which suggests that dislocations or defects produced by movement of the dislocations are responsible for the color (Collins et al.,

2000). However, analysis of the dislocation densities (~10^9/cm^2) and their expected absorption strengths indicates that they alone cannot account for the observed color intensities (Fall et al., 2002; Willems et al., 2006; Mäki et al., 2007; Fisher et al., 2009). Other studies have proposed that the brown color is produced by absorption from vacancy clusters or {111}-oriented vacancy discs also found in heavily distorted regions of the diamond lattice (Avalos and Dannefaer, 2003; Hounsome et al., 2006; Bangert et al., 2009). The presence of clusters in brown natural diamond has been confirmed by positron annihilation experiments, which demonstrated that the smaller clusters are optically active. These clusters have been shown to anneal out and/or aggregate to form larger, optically inactive clusters at the HPHT annealing temperatures (up to ~2500°C) required to remove brown color from natural diamond (Avalos and Dannefaer, 2003; Fisher et al., 2009).

In Brief

- Gemesis Corp. has sold mounted and loose CVD synthetic diamonds since March 2012.
- The latest generation products examined for this report ranged up to 0.90 ct, and most were near-colorless and had clarity grades between IF and VVS; all but one were round brilliants.
- Spectroscopic evidence indicates a likelihood that these CVD synthetics have undergone post-growth HPHT processing to enhance their color and possibly their clarity.
- This material is conclusively identified by PL spectroscopy and DiamondView fluorescence images.

X-ray topography of brown single-crystal as-grown CVD synthetic diamond has not shown significant plastic deformation (Martineau et al., 2004). Dislocations in CVD material appear to have nucleated at the interface with the substrate, thus forming approximately perpendicular to the growth surface (Martineau et al., 2004, 2009). The dislocation densities in as-grown CVD synthetic diamond are relatively low (~10^4–10^6/cm^2) and thus are not considered the main cause of brown color. Positron annihilation studies have shown that brown as-grown CVD synthetics may contain vacancy clusters of various sizes, ranging from monovacancies to nanometer-size voids (Mäki et al., 2007). The smaller clusters anneal out in a temperature range (1400–1600°C) similar to that at which the brown color is removed in CVD synthetic diamond (Charles et al., 2004; Martineau et al., 2004; Mäki et al., 2007). Yet it has not been conclusively demonstrated that these clusters are responsible for coloration, especially as several other point defects in CVD synthetic diamond are created and destroyed at these temperatures. The difference in the temperature stability of color-causing defects between natural and CVD synthetic brown diamond is not yet understood, and theoretical and experimental studies are ongoing.

Gem-quality CVD specimens with post-growth treatments have occasionally been submitted to gem laboratories for grading (Chadwick, 2008a,b). The purpose of the treatment is not limited to changing the color from brown to colorless, as intense pink CVD synthetic diamonds from Apollo (Wang et al., 2010) have also shown evidence of treatment with multiple steps.

MATERIALS AND METHODS

For this investigation, we purchased 16 faceted CVD synthetic diamonds from Gemesis (table 1; see also figure 1). These ranged from 0.24 to 0.90 ct, with an average weight of 0.46 ct. The majority (94%) were cut as round brilliants, with depths of 2.41 to 3.69 mm, averaging 2.93 mm. These CVD synthetics are representative of the current production being sold on the Gemesis website.

Experienced members of GIA's diamond grading staff determined color and clarity grades using GIA's grading system. Internal features were examined with a standard gemological binocular microscope and a research-grade Nikon microscope, using a variety of lighting techniques, including darkfield and fiber-optic illumination and polarization. Reactions to UV radiation were tested in a darkened room with a conventional 4 watt combination long-wave (365 nm) and short-wave (254 nm) UV lamp. We also examined the samples for fluorescence, phosphorescence, and crystal growth characteristics using the Diamond Trading Company (DTC) DiamondView instrument (Welbourn et al., 1996). Phosphorescence images were collected with a 0.1 second delay and 5 seconds of exposure time.

Phosphorescence spectra were collected on all samples at room temperature with an Ocean Optics HR4000 spectrometer. After illuminating the samples for 30 seconds with an Avantes AvaLight-DH-S deuterium-halogen light source (emission wave-

TABLE 1. CVD synthetic diamonds from Gemesis Corp. examined in this study.

Sample	Weight (ct)	Color	Cut	Clarity	UV fluorescence		N_S^0 (ppb)	$[NVH]^-$ (ppb)
					Long-wave	Short-wave		
GS02	0.30	G	Round	VVS_1	Inert	Very weak green	na[a]	na
GS03	0.41	F	Round	VVS_2	Inert	Very weak green	na	na
GS04	0.26	G	Round	VVS_1	Very weak green	Weak green	na	na
GS05	0.31	G	Round	IF	Inert	Very weak green	na	na
GS06	0.24	G	Round	VS_1	Inert	Very weak green	na	na
GS07	0.24	F	Round	VVS_2	Inert	Very weak green	72 ± 10	<5
GS08	0.39	F	Round	VVS_2	Inert	Very weak green	170 ± 25	<10
GS09	0.48	G	Round	VS_1	Inert	Weak green	180 ± 20	<10
GS10	0.41	G	Round	VVS_1	Very weak green	Weak green	180 ± 20	<10
GS11	0.47	G	Round	VVS_2	Very weak green	Weak green	150 ± 20	<5
GS12	0.47	I	Round	VS_1	Very weak green	Weak green	220 ± 30	<10
GS13	0.47	G	Round	VVS_1	Inert	Very weak green	170 ± 25	<10
GS14	0.39	G	Round	VS_2	Inert	Weak green	150 ± 20	<5
GS15	0.70	I	Round	VVS_2	Weak green	Moderate green	280 ± 40	<10
GS16	0.83	J	Round	VVS_2	Inert	Weak green	340 ± 30	<10
GS17	0.90	L	Rectangle	VVS_2	Very weak green	Weak green	450 ± 50	<15

[a] *Abbreviation: na = not analyzed.*

length of 215–2500 nm), we began data collection. A 1 second spectral integration time was used, and data collection continued for 60–100 seconds.

Infrared absorption spectroscopy of all samples was performed in the mid-IR (6000–400 cm^{-1}, at 1 cm^{-1} resolution) and near-IR (up to 11,000 cm^{-1}, at 4 cm^{-1} resolution) ranges at room temperature with a Thermo Nicolet Nexus 6700 Fourier-transform infrared (FTIR) spectrometer equipped with KBr and quartz beam splitters. Samples were first cleaned in an ultrasonic bath of acetone and dried with compressed air. A DRIFT (diffuse reflectance infrared Fourier transform) unit focused the incident beam on the sample, and up to 256 spectral scans were averaged for increased signal-to-noise ratios. Additionally, the sample chamber was purged with nitrogen gas. The mid- and near-IR spectra were normalized relative to the two- and three-phonon diamond absorptions, enabling quantitative analysis of impurity-related peak intensities.

Continuous-wave electron paramagnetic resonance (EPR) was used to investigate paramagnetic point defects (see box A) in 11 of the samples. Spectra were acquired at room temperature using a commercial X-band (~9.7 GHz) Bruker EMX-E spectrometer equipped with a super-high-Q (SHQ) spherical resonant cavity and a Bruker ER 041 XG-H microwave bridge. The samples were held in dual-axis goniometers that enabled accurate positioning within the EPR cavity. Further details regarding signal optimization and the simulation and fitting of EPR spectra of paramagnetic defects is described by Edmonds et al. (2008). Defect concentrations in the study samples were calculated by comparing their EPR-integrated intensities to those of a type Ib HPHT synthetic diamond (single growth sector) reference sample with a known concentration of neutral single-substitutional nitrogen (N_S^0). The N_S^0 concentration of this sample was originally determined using EPR and infrared absorption spectroscopy.

Absorption spectra in the ultraviolet through visible to near-infrared range (UV-Vis-NIR, 250–1000 nm) were recorded on all samples with a custom-built instrument using an Avantes AvaSpec-2048 spectrometer and two broadband light sources (AvaLight-HAL and AvaLight-DH-S). This high-resolution apparatus enabled the detection of very weak and sharp absorptions at liquid-nitrogen temperature (77 K). The sampling interval in this four-channel device was 0.04–0.07 nm, depending on the specific wavelength ranges, with a 10 µm entrance slit width. Using 200 scans per spectrum, we achieved spectral resolution better than 0.2 nm, as well as a very good signal-to-noise ratio. Samples were immersed in a specially designed bath containing multiple layers of liquid

BOX A: ELECTRON PARAMAGNETIC RESONANCE OF POINT DEFECTS IN DIAMOND

EPR spectroscopy is an extremely sensitive quantitative tool for chemical and structural identification of paramagnetic point defects in diamond and other nonmetallic materials. A paramagnetic defect in diamond, such as the single substitutional nitrogen center (N_S^0 or C-center), contains one or more unpaired electrons. An electron has an intrinsic magnetic moment, which can be visualized as a small bar magnet or compass needle. This magnetic moment arises from the quantum mechanical property called *spin* (*S*). Thus, EPR is also known as electron spin resonance (ESR). An electron has an intrinsic spin $S = ½$. In systems containing more than one electron, the resultant total spin can be zero (i.e., two electrons in a chemical bond) or non-zero. In diamond, covalent bonds are formed between neighboring carbon atoms. Each carbon atom has four electrons available for bonding and "points" four hybrid atomic orbitals at neighboring atoms. These orbitals on neighboring atoms interact, producing bonding and anti-bonding molecular orbitals between neighbors. Each bonding molecular orbital accommodates two anti-parallel paired electrons (a consequence of the Pauli Exclusion Principle) with an overall spin $S = 0$ (figure A-1, left). The covalent bonds produced by the carbon atoms sharing electrons are very strong. The anti-bonding orbital is much higher in energy and is empty. Thus pure diamond is not EPR-active.

Nitrogen contains one more electron than carbon, and when it substitutes for a carbon atom in the diamond lattice (N_S^0), it can bond with neighboring carbons, but one electron is left over, resulting in an overall spin of $S = ½$. This lone electron is accommodated in an anti-bonding orbital formed between the nitrogen and one of its carbon neighbors. This unpaired electron has two spin states split by a magnetic field, the lower energy one corresponding to the magnetic moment of the electron parallel to the applied field, and the upper one anti-parallel (figure A-1, right). The interaction between the applied magnetic field and the electron spin (magnetic moment) is known as the (anomalous) *Zeeman effect*. Magnetic dipole transitions between the two spin states can be driven with microwave radiation that matches the energy separation. Usually the magnetic field is swept (i.e., increased or decreased in a swift manner across a chosen magnetic field range) to produce an EPR spectrum; when the energy of the fixed frequency microwave radiation matches the separation of the levels, an EPR signal is observed.

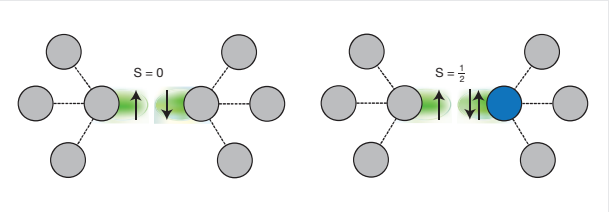

Figure A-1. Pure diamond is not EPR-active because each bonding molecular orbital accommodates two anti-parallel paired electrons with an overall spin S = *0 (left). When a nitrogen atom substitutes for a carbon atom in the diamond lattice (N_S^0) the additional electron is accommodated in an anti-bonding orbital formed between the nitrogen and one of its carbon neighbors. This unpaired electron has a spin* S = *½, so N_S^0 is EPR-active (right).*

Fortunately, an unpaired electron is highly sensitive to its environment, and it is these interactions that produce more complex spectra with a wealth of information about the nature and constituents of the defects under investigation. For example, an unpaired electron can interact with neighboring nuclei that possess nuclear spin. This produces a local magnetic field, which will have the effect of either increasing or decreasing the effective magnetic field experienced by the unpaired electron, depending on the relative orientation of the two spins. Consequently, additional "satellite" resonance lines due to nuclei with nuclear spin will appear about the center of the spectrum.

EPR has a very high sensitivity, and N_S^0 defect concentrations of ~1 ppb can be routinely measured in minutes. Usually the spectra contain overlapping contributions from several defects, but these can be deconvolved, facilitating detailed quantitative analysis even when multiple defect species are present in the same sample.

nitrogen (patent pending), ensuring consistent temperature and a stable environment free of nitrogen gas bubbles.

A commercial Renishaw InVia Raman confocal microspectrometer, equipped with the liquid nitrogen bath setup used for UV-Vis-NIR spectroscopy, was used for low-temperature photoluminescence (PL) spectral analysis of all samples. Various defect centers were excited using five excitation wavelengths produced by four laser systems. An Ar-ion laser was operated at excitation wavelengths of 488.0 nm (for the 490–850 nm range) and 514.5 nm (for the 517–850 nm range). PL spectra were collected in the 640–850 nm range using an He-Ne laser (632.8 nm), and in the 835–1000 nm range using a diode laser (830.0 nm). In addition, an He-Cd metal-vapor laser (324.8 nm) was used for the 370–800 nm range. Up to three scans were accumulated for each spectrum to improve the signal-to-noise ratio.

Figure 2. Internal features in the CVD synthetic diamonds consisted of small (generally <50 µm) irregular black inclusions (left, image width 1.0 mm), likely composed of non-diamond carbon. Radial fractures surrounded some of the larger inclusions (right, image width 1.3 mm), a result of strong, highly localized strain. Photomicrographs by W. Wang.

RESULTS

Color and Shape. Three of the 16 samples were graded as colorless (F color) and 12 as near-colorless (G–J; see table 1). Only one was faintly colored (L), with the color falling within the yellow hue range. The three largest diamonds had the poorest color grades. The largest sample (0.90 ct) was the only one polished into a rectangular shape; the other 15 samples were round brilliants.

Clarity. The samples showed very high clarity (again, see table 1). Twelve of them had clarity grades between IF and VVS. This marked the first time GIA has given an IF grade to a CVD synthetic diamond (sample GS05, 0.31 ct). Only four samples fell in the VS category. Clarity grades in those samples were lowered by small black inclusions with irregular shapes (probably non-diamond carbon; figure 2). Most of these inclusions were smaller than 50 µm. Small petal-shaped radial fractures were occasionally observed around some of the larger inclusions. It is noteworthy that none of the samples contained noticeable fractures.

Birefringence. Dislocation-related graining is a common feature in many CVD synthetics. Nevertheless, graining was not observed in these Gemesis samples. Microscopic imaging with crossed polarizers did reveal relatively weak anomalous double refraction patterns compared with those of CVD samples in previous studies (Wang et al., 2003, 2005, 2010). These irregular, linear, or occasionally "tatami" patterns were characterized by low-order interference colors, including gray and blue (figure 3, left and center). Extremely high-order interference colors with characteristic symmetrical patterns were only observed around small black inclusions, a good indication of increased strain in highly localized regions (figure 3, right).

Fluorescence and Phosphorescence. A remarkable property of the Gemesis synthetics was their response to UV radiation (table 1). Unlike the orange-red fluo-

Figure 3. Relatively weak anomalous double refraction was seen when viewing these synthetic diamonds with crossed polarizers, showing low-order gray and blue interference colors with irregular, linear, or occasionally "tatami" type patterns (left and center, image widths 3.3 and 3.1 mm, respectively). Petal-shaped regions of birefringence with characteristic symmetrical patterns were sometimes observed around small black inclusions (right, image width 0.9 mm). Photomicrographs by W. Wang.

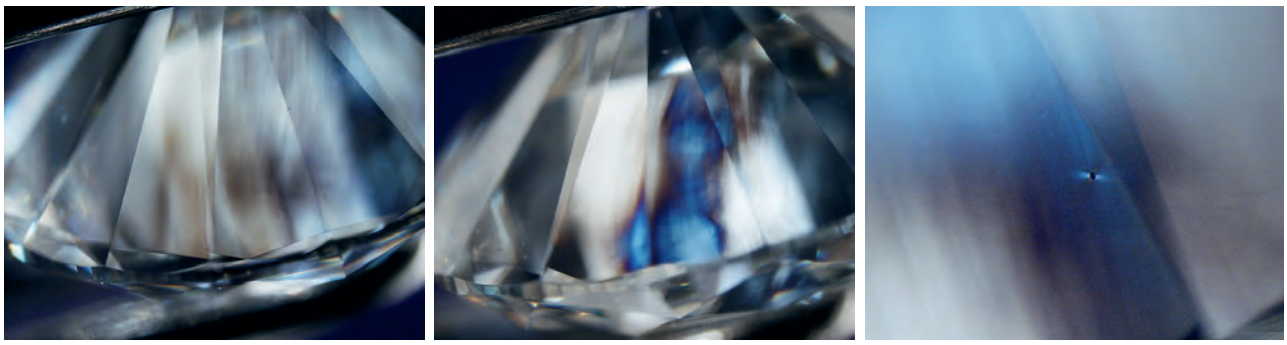

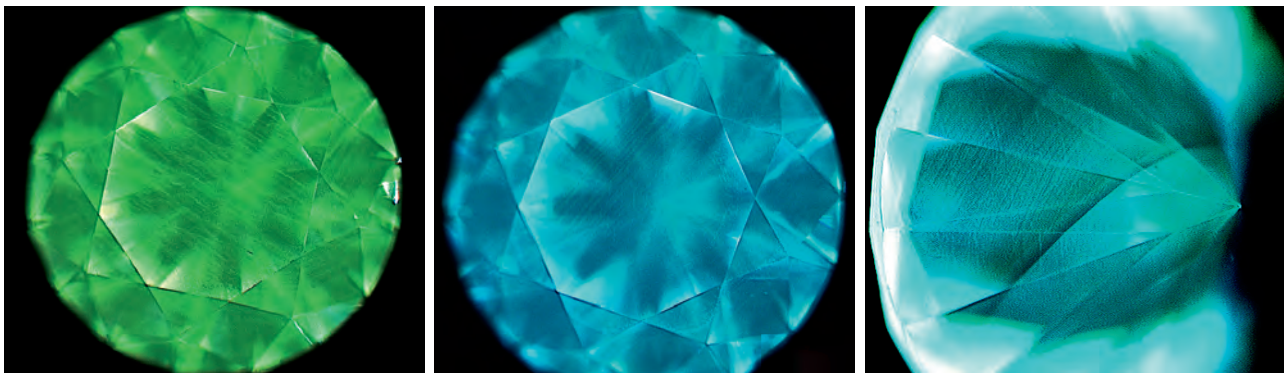

Figure 4. In the DiamondView, three of the synthetic diamond samples were dominated by green fluorescence (e.g., left, 0.30 ct). Four showed strong blue fluorescence (center, 0.47 ct), and the other samples showed transitional features. Even in those dominated by blue fluorescence, the green striations were still clearly observable. In 12 of the 16 samples, the DiamondView revealed a sharp, well-defined fluorescence boundary with a ~45° angle to the table face (right, 0.41 ct). One side of the boundary showed normal green-blue fluorescence, while the other had much weaker fluorescence. Images by W. Wang.

rescence commonly associated with CVD material, the samples in this study displayed green fluorescence (mostly of weak to very weak intensity) to short-wave UV. Additionally, six samples fluoresced weak to very weak green when exposed to long-wave UV radiation, while the remainder were inert.

The high-intensity ultra-short UV wavelength of the DTC DiamondView (~225 nm radiation) revealed growth striations in all the samples, with green fluorescence of varying intensity. An alternating pattern of very narrow green striations was occasionally distributed throughout the whole specimen (figure 4, left). Three of the synthetics were dominated by green fluorescence and four showed strong blue fluorescence, while other samples showed transitional features. Even in those dominated by blue fluorescence, the green striations were still clearly visible (figure 4, center). In 12 of the 16 samples, the DiamondView fluorescence image also revealed a sharp, well-defined boundary separating areas showing dominant green fluorescence or where the fluorescence was significantly weaker or nearly undetectable (figure 4, right). Similar banding structures were reported in Apollo CVD synthetics (e.g., Wang et al., 2010), but with a different orientation of the bands relative to the table facet. The bands in the Apollo samples were mostly aligned parallel to the table, while those in Gemesis samples intersected the table at ~45°. The four samples in this study that did not show the banding structure were among the smallest pieces (0.24–0.31 ct).

The Gemesis CVD synthetics displayed evenly distributed blue phosphorescence of varying inten-

Figure 5. Blue phosphorescence with varying intensity, observed in the DiamondView, was distributed evenly throughout each of the synthetic diamonds, as shown here for samples weighing 0.26, 0.39, and 0.24 ct. Images by W. Wang.

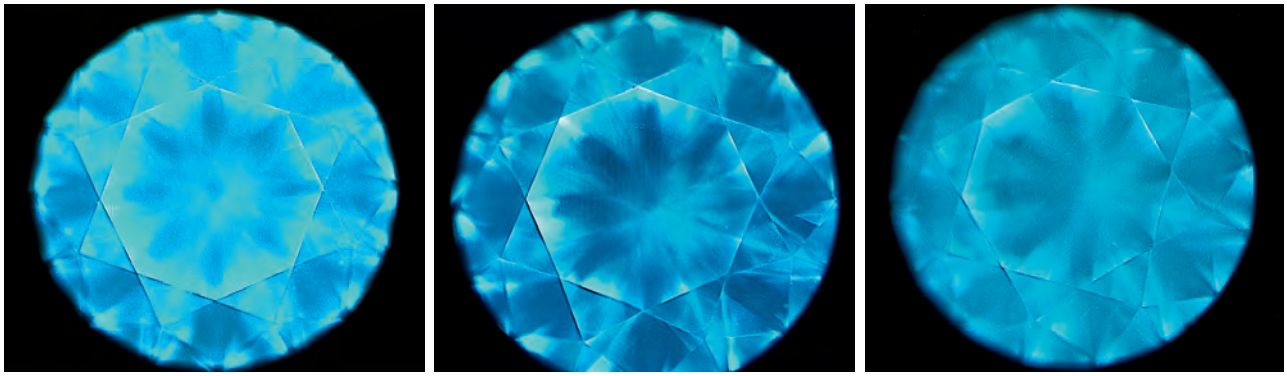

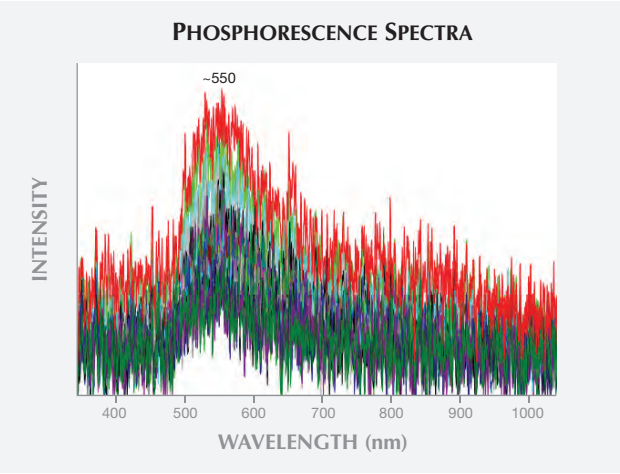

Figure 6. The five synthetic diamonds that showed strong phosphorescence in the DiamondView had a broad but clear band centered at ~550 nm in their phosphorescence spectra.

sity (figure 5). Only weak phosphorescence was observed in the samples dominated by green fluorescence. The phosphorescence was markedly stronger in those that displayed intense blue fluorescence. Phosphorescence spectra were dominated by a broad band centered at ~550 nm, which was best defined in the samples that showed strong emissions in the DiamondView (figure 6).

Infrared Absorption Spectroscopy. The Gemesis samples displayed relatively featureless absorption spectra in the infrared region, unlike those reported in CVD synthetics from other sources (Wang et al., 2003, 2005, 2010; Martineau et al., 2004). Defect-related absorptions were only observed in the 1500–1100 cm^{-1} region. These features (e.g., figure 7) included a relatively sharp peak at 1332 cm^{-1} and another peak at 1344 cm^{-1}, both attributed to different charge states of the single substitutional nitrogen defect. The 1332 cm^{-1} absorption is due to the positive charge state, N_S^+ (Lawson et al., 1998), while the 1344 cm^{-1} line is associated with the neutral charge state, N_S^0 (Collins et al., 1987).

While the 1332 cm^{-1} peak was recorded in each sample, the 1344 cm^{-1} peak was not detected in two of them (GS02 and GS07). The intensity of the 1344 cm^{-1} absorption varied from sample to sample, but generally fell below 0.01 cm^{-1}, corresponding to an N_S^0 concentration of <1 ppm carbon atoms. Interestingly, we did not detect the 3123 cm^{-1} local vibration mode attributed to the neutral charge state of the nitrogen vacancy-hydrogen-complex $[N\text{-}V\text{-}H]^0$, as reported previously in CVD synthetic diamond (Fuchs et al., 1995a,b; Wang et al., 2003; Martineau et al., 2004; Khan et al., 2009, 2010; Liggins, 2010). Furthermore, the absorption line at 3107 cm^{-1}, which can sometimes be introduced into a brown CVD synthetic after HPHT treatment, was not observed (Charles et al., 2004; Martineau et al., 2004). Spectroscopy in the near-infrared region did not reveal any other absorption peaks previously reported in CVD synthetics, such as lines at 8753, 7354, 6856, 6524, and 5564 cm^{-1} (Wang et al., 2003; Martineau et al., 2004).

Electron Paramagnetic Resonance Spectroscopy. EPR spectroscopy is useful for identifying the presence of CVD-specific paramagnetic defects (e.g., Glover et al., 2003, 2004; Edmonds et al., 2008; D'Haenens-Johansson et al., 2010, 2011). This technique can be used to quantify the concentrations of N_S^0 (Smith et al., 1959; Cox et al., 1994) and the negatively charged state of the nitrogen-vacancy-hydrogen defect ($[N\text{-}V\text{-}H]^-$; Glover et al., 2003); results for the 11 Gemesis samples tested are reported in table 1. The EPR spectrum for GS11, shown in figure 8, is representative of the samples. The N_S^0 concentrations ranged from as low as 72 ± 10 ppb (GS07, F color) to as high as 450 ± 50 ppb (GS17, L color). The average concentration was 215 ppb, with a standard deviation of 105 ppb. Although there was not a wide distribution of color grades for the samples tested (F–L, with 45% having a G color), comparison between the grades and the N_S^0 concentrations suggest that as the concentration increased the grade fell lower on the color scale. This is understandable, since isolated nitrogen is known

Figure 7. Absorption spectra of the Gemesis synthetic diamonds in the middle and near-infrared regions are very "clean." Only weak absorptions at 1344 and 1332 cm^{-1} (due to isolated nitrogen) were detected in some samples. Spectra are shifted vertically for clarity.

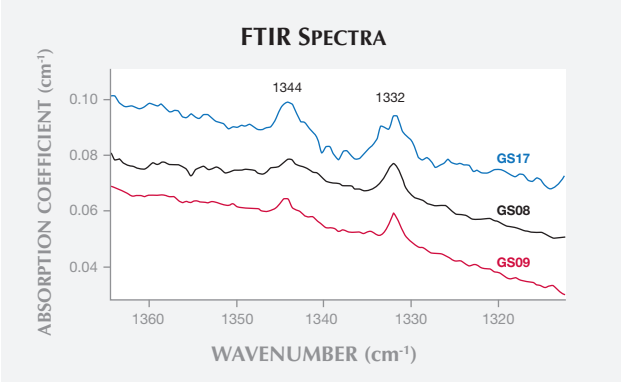

to impart yellow color in diamond. The $[N\text{-}V\text{-}H]^-$ center was not detected by EPR, with upper concentration limits ranging from 5 to 15 ppb (table 1).

UV-Vis-NIR Absorption Spectroscopy. Since the faceting of the samples made it impossible to accurately determine the pathlength of the beam, the absorbance of the samples could not be converted into absorption coefficients, as was done with the FTIR absorption data, limiting quantitative data analysis. Nevertheless, several absorption features were identified, indicating the presence of certain impurity defects.

A gradual, shallow increase was observed in the absorption spectra from approximately 300 nm down to the diamond absorption edge at ~225 nm (figure 9A). Defect-related absorptions were detected in the infrared and deep-UV regions, with the visible region (400–700 nm) appearing featureless. Notably absent were the absorption lines at 586 nm (different from the 596/597 nm doublet sometimes observed in PL) and 625 nm, which have been reported in some brown CVD synthetics (Wang et al., 2003; Martineau et al., 2004).

A broad absorption band centered at ~270 nm and sharp peaks at 271.5 and 268.0 nm were detected in all of the samples (again, see figure 9A). These absorptions are attributed to the isolated nitrogen impurity in diamond (Dyer et al., 1965). The intensity of these absorption peaks varied significantly, though they were more pronounced in samples with higher N_S^0 concentrations. It is noteworthy that the ~270 nm band was detectable even in samples with very low nitrogen concentrations, such as GS07 (72 ± 10 ppb). This synthetic diamond had a relatively low carat weight (0.24 ct), so its path length was not expected to be longer than that of the others, which might have skewed the results. These observations demonstrated the effectiveness of UV-Vis-NIR absorption spectroscopy in detecting traces of isolated nitrogen, even in samples weighing ~0.5 ct. Readily detectable N_S concentrations are rare in natural diamonds.

An absorption doublet at 736.6 and 736.9 nm (figure 9B) was detected in 14 of the samples (absent from GS11 and GS17). This feature, which was active in both absorption and luminescence, has been attributed to the negative charge state of the silicon split-vacancy center, $[Si\text{-}V]^-$ (Vavilov et al., 1980; Clark et al., 1995; Goss et al., 1996). The $[Si\text{-}V]^-$ center is frequently observed in the absorption and PL spectra of CVD synthetics (Wang et al., 2003, 2005, 2007; Martineau et al., 2004). The strongest $[Si\text{-}V]^-$ absorbance was recorded in

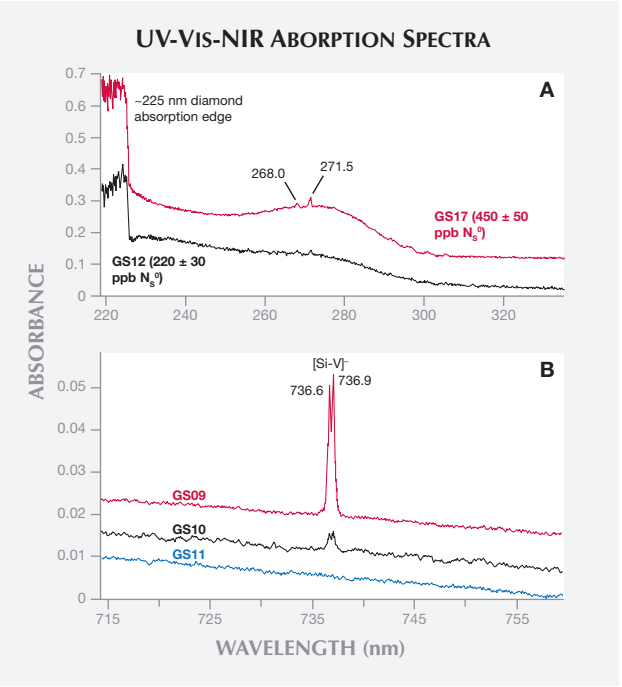

Figure 9. UV-Vis-NIR absorption spectroscopy of the Gemesis synthetic diamonds at liquid-nitrogen temperature revealed a broad absorption band centered ~270 nm from isolated nitrogen in every sample (A). Sharp doublet absorptions at 736.6/736.9 nm from the $[Si\text{-}V]^-$ center were present in most samples (B). Spectra are shifted vertically for clarity.

Figure 8. The EPR spectrum of sample GS11 (labeled "experimental") shown here is representative of all the analyzed Gemesis samples and was taken with the magnetic field along [111]. The relative intensities and positions of the spectral lines agreed with those of the simulated spectrum for N_S^0, identifying the paramagnetic species and allowing the determination of N_S^0 concentrations (see table 1). No other paramagnetic defects were detected.

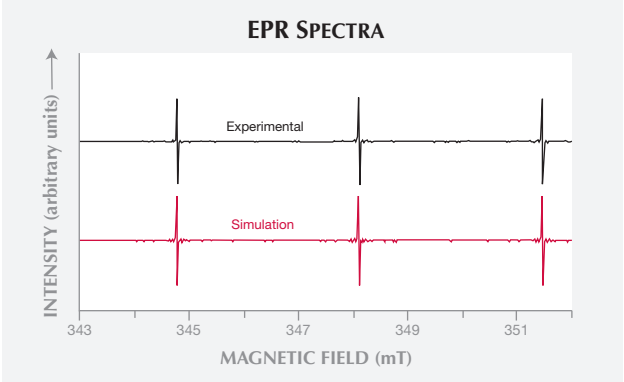

samples GS03, GS08, GS09, and GS14. Even so, there was no clear correlation between diamond color grades and concentrations of Si-related defects.

Photoluminescence. With an appropriate excitation wavelength, the detection limit for optical emission peaks from luminescence defects may be significantly lower than that for their absorption peaks, revealing the presence of otherwise unexpected defects. The excitation efficiencies of the zero phonon lines (ZPLs) depend on the excitation wavelength chosen. Therefore, five different excitations were used to collect PL spectra, spanning the ultraviolet through infrared regions, so certain emission centers were detected under multiple excitation conditions. The major PL features are summarized below on the basis of individual laser excitation in each defect's most sensitive region.

The PL spectra acquired using 514.5 nm (green) laser excitation are shown in figure 10A. The ZPL emissions for $[Si\text{-}V]^-$ (736.6/736.9 nm doublet) and nitrogen-vacancy centers in neutral ($[N\text{-}V]^0$ at 574.9 nm) and negative ($[N\text{-}V]^-$ at 637.0 nm) states dominated the spectra. A broad asymmetric band at 766 nm was also observed. This band is part of the vibronic structure of $[Si\text{-}V]^-$, and thus the feature's intensity correlated with that of the $[Si\text{-}V]^-$ ZPL (Clark and Dickerson, 1991). In 13 of the samples (81%), the 637.0 nm ZPL was more intense than the 574.9 nm peak, with a ratio ranging from 1.09 to 2.97. For the three remaining samples (GS10, GS12, and GS14), this ratio fell in the 0.44–0.99 range. A doublet emission at 596.5 and 597.0 nm, previously documented as a common feature of colorless, near-colorless, and brown as-grown CVD synthetics (Wang et al., 2003, 2007; Martineau et al., 2004), was not observed in these Gemesis samples. Numerous emission peaks were also observed in the 520–580 nm region, including peaks at 525.4, 535.1, 540.4, 546.1, and 572.9 nm (figure 10B). The defects responsible for these emission lines have not been identified.

Figure 10. In photoluminescence spectra of the Gemesis synthetic diamonds collected with 514.5 nm laser excitation at liquid-nitrogen temperature, emissions from N-V and $[Si\text{-}V]^-$ centers were observed in each sample (A). Numerous sharp peaks were recorded in the 520–580 nm region, including major ones at 525.4, 535.1, 540.4, 546.1, and 572.9 nm (B). The assignment of these emissions remains unclear.

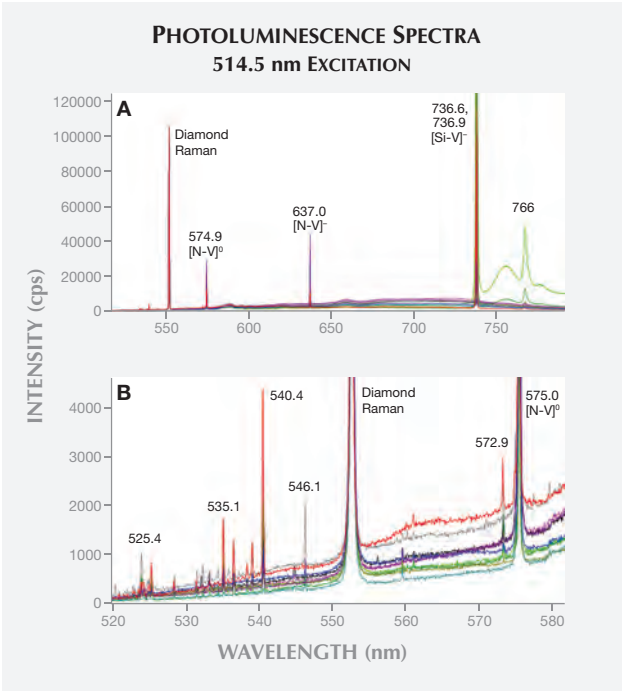

ZPL widths are sensitive to lattice dislocations in diamond, widening with increased local strain. Fisher et al. (2006) reported the effective use of the full width at half maximum (FWHM) of the neutral vacancy defect (GR1) in probing the strain in natural and HPHT-processed natural diamonds. GR1 is not detected in CVD synthetic diamond unless irradiated, so this feature could not be used to characterize the strain of the samples in this study. However, Fisher et al. (2006) also noted that the FWHM for the N-V peaks corresponded with those measured for GR1 (in milli-electron volts). For the Gemesis samples in our investigation, the FWHM of the 574.9 nm peak showed a limited variation of 0.20–0.30 nm, with an average of 0.24 nm. In contrast, the FWHM of the 637.0 nm emission line varied from 0.16 to 0.33 nm, with an average of 0.21 nm. In these samples, a positive correlation existed between widths of these two peaks, and their plots overlapped the narrowest FWHM data for natural type IIa diamonds (figure 11). In contrast, the same peaks in both pink and colorless CVD synthetics by Apollo (Wang et al., 2007, 2010, and unpublished data) are much broader than those of the Gemesis CVD samples we studied, and overlap the broad FWHM data of natural type IIa diamonds.

The PL spectra taken with 324.8 nm laser excitation are shown in figure 12. This laser wavelength excited a very weak luminescence line at 415 nm in nine of the samples (56%). This line has been attributed to the N3 defect in diamond, which consists of three nitrogen atoms in a {111} plane, bonded to a single vacancy (Davies, 1974; Davies et al., 1978; Mar-

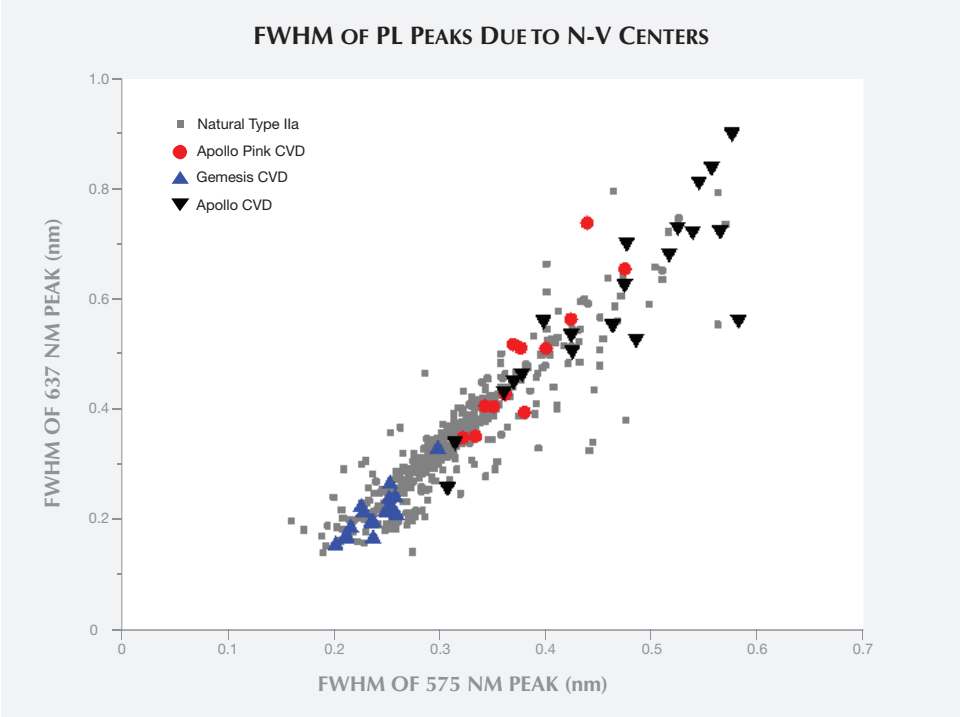

Figure 11. The width of the PL peaks due to N-V centers in the Gemesis synthetic diamonds overlapped the narrowest values in natural type IIa diamonds. These peaks in the Gemesis CVD synthetics were clearly narrower than those documented in Apollo samples.

tineau et al., 2004). An additional series of lines in the 451–459 nm range was detected in all of the samples; these were previously reported in HPHT-processed CVD synthetics by Martineau et al. (2004). These lines have not been reported in natural diamond.

PL spectra collected using blue laser (488.0 nm) excitation revealed a relatively strong emission at 503.2 nm, attributed to the H3 defect (figure 13). Many unidentified sharp peaks were recorded in the 495–535 nm region. Several of them, including a 524.5 nm peak, were excited by both the 488.0 nm and 514.5 nm lasers. These are probably part of all sharp emissions that continuously spread from 580 nm to the high-energy side; the 520–580 nm region was recorded in 514.5 nm laser excitation PL spectra (figure 10B).

The only features detected using 633.0 nm laser excitation were the 736.6/736.9 nm doublet from the

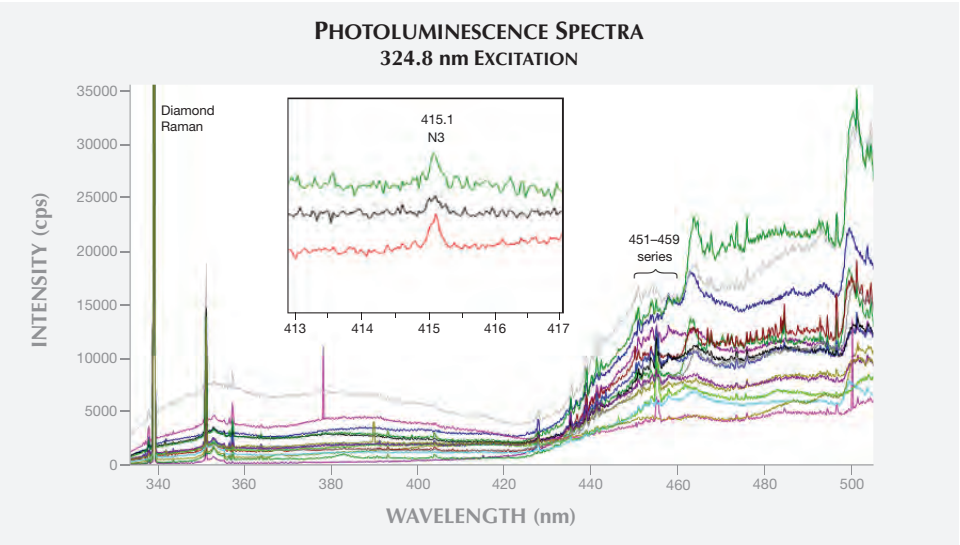

Figure 12. A weak emission at 415.1 nm from the N3 optical center was detected in many of the Gemesis synthetic diamonds using 324.8 nm laser excitation.

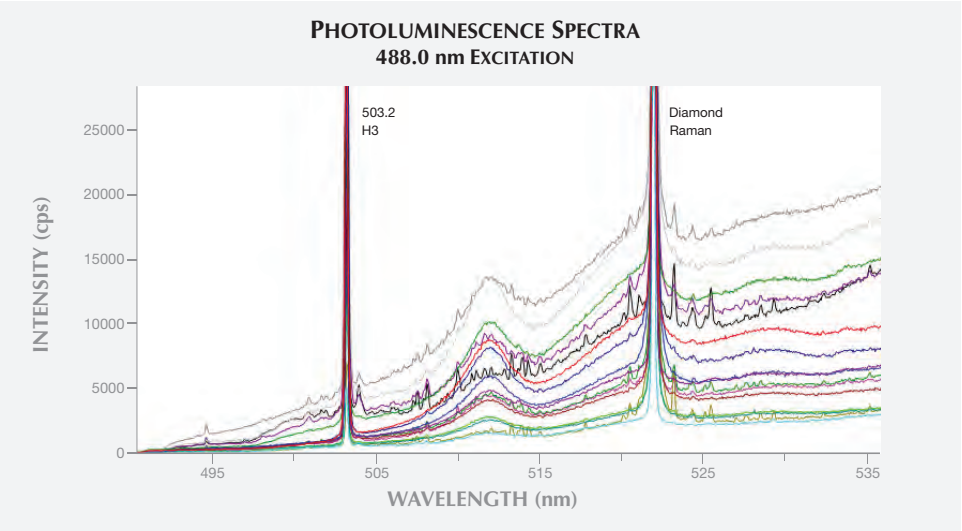

Figure 13. The dominant feature in PL spectra of the Gemesis CVD samples with 488.0 nm laser excitation is the strong H3 emission, responsible for the green fluorescence to short-wave UV radiation observed in all 16 samples.

[Si-V]$^-$ center and the corresponding vibronic structure (figure 14).

PL ZPLs at 850.0 and 875.5 nm were detected in all of the samples when excited with an 830.0 nm laser. Furthermore, a 946.0 nm emission was observed in five of them (figure 15). This ZPL has been attributed to the neutral charge state of the silicon split-vacancy defect, [Si-V]^0 (D'Haenens-Johansson et al., 2010; 2011). In addition, sample GS14 displayed emissions at 882.7 and 884.4 nm. Both the peak positions and their relative intensities agree with those assigned to nickel-related centers.

Although only semiquantitative analysis of the PL and absorption data was possible, the presence of certain optical centers could be determined. It was noted that the samples with relatively high concentrations of Si-related defects, characterized by strong [Si-V]$^-$ absorption, also showed emission lines at 946 nm ([Si-V]^0) and 766 nm. The intensity of the 850.0 and 875.5 nm emissions also showed a positive correlation with the 946 nm line.

DISCUSSION

Progress in Quality of Synthetic CVD Gem Diamonds. CVD synthetic diamonds produced for the jewelry market have shown significant improvement in the past decade. The early products from Apollo

Figure 14. Emissions recorded in the Gemesis synthetic diamonds with 633.0 nm laser excitation consisted of a 736.6/736.9 nm doublet from the [Si-V]$^-$ defect and a broad peak at 766 nm. This confirmed the positive correlation in peak intensities between the [Si-V]$^-$ emission and the 766 nm peak, also observed with 514.5 nm laser excitation.

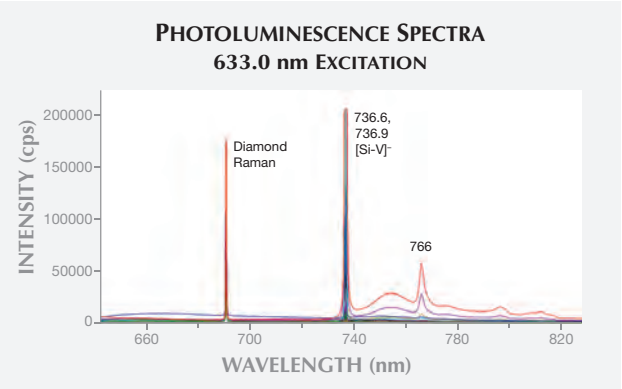

Figure 15. With 830.0 nm laser excitation, PL emissions at 850.0 and 875.5 nm were recorded in each of the Gemesis synthetic diamonds. Also observed in five samples was the [Si-V]^0 emission at 946.0 nm. Sample GS14 also displayed 882.7 and 884.4 nm emissions from well-known Ni-related defects. The spectrum for GS14 is shifted vertically for clarity.

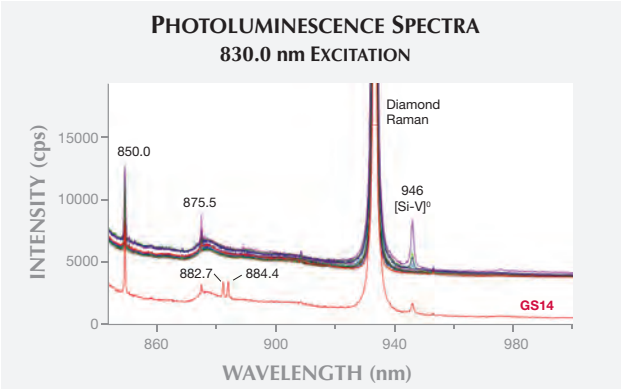

(Doering and Linares, 1999; Linares and Doering, 1999; Wang et al., 2003) consisted of relatively thin plates and the faceted gems were small, with distinct and sometimes intense brown coloration. Inclusions were common, resulting in medium or low clarity grades such as SI and I. Although the color and clarity of Apollo's products improved over time, their size (0.15–0.30 ct) was still limited by the achievable table-to-culet depths and by cut grading considerations (Wang et al., 2007). The Gemesis CVD samples in this study had high color and clarity grades, with most being colorless or near-colorless and VVS or better. Sample GS05 (0.31 ct) is the first documented faceted CVD synthetic diamond with IF clarity. Moreover, the average carat weight of the samples we examined, 0.46 ct, falls within the range of the most popular diamond weights in the market. We can expect even better gem-quality CVD products as synthesis methods continue to improve. In fact, CVD could become the preferred method for growing colorless gem diamonds commercially. The HPHT growth of colorless or near-colorless gem diamonds continues to face the challenges of effectively preventing isolated nitrogen from entering the diamond lattice, and keeping metallic catalysts/solvents from being incorporated as inclusions. Both of these factors require a reduction in the synthetic diamond growth rate under HPHT conditions.

Spectroscopic Features and Possible Post-Growth Treatment. Previously documented as-grown CVD synthetic diamonds were colorless, near-colorless, or (most often) some shade of brown (Martineau et al., 2004; Wang et al., 2007). Specific absorptions in the mid-IR and near-IR regions and doublet emissions at 596.5 and 597.0 nm are important for separating as-grown CVD synthetics from natural diamonds. These centers are formed during synthesis but may, under the right conditions, be destroyed by post-growth treatments. Such enhancements may be revealed by the introduction of defects not observed in as-grown CVD material.

The Gemesis products in this study had a distinctly different combination of lattice defects from as-grown CVD synthetics. Their absorption spectra in the mid- and near-IR regions were surprisingly featureless, and the 3123 cm^{-1} band was notably absent from every sample. Only weak absorptions at 1344 and 1332 cm^{-1} due to isolated nitrogen were observed in some samples' FTIR spectra.

Similarly, the UV-Vis-NIR absorption spectra differed from those of conventional CVD synthetics. There was a gradual, generally featureless increase in absorption from ~700 nm down to the diamond edge at ~225 nm (from lower to higher energies). Absorption features that are characteristic of as-grown CVD samples, such as the 596 and 625 nm (Martineau et al., 2004), were not detected.

H3 Center. PL spectroscopy using 488.0 nm laser excitation revealed the presence of the H3 defect (503.2 nm) in all of the Gemesis samples. (The H3 concentration was below the detection limit for UV-Vis-NIR absorption.) When excited, the H3 defect emits green light centered at ~520 nm; this defect is responsible for the green fluorescence excited by the short-wave UV lamp and the DiamondView (figure 4). The low-temperature synthesis conditions of the CVD method are not favorable for the production of multi-nitrogen defects such as H3 ($[N\text{-}V\text{-}N]^0$). Instead, nitrogen impurities in as-grown CVD synthetic diamond usually exist in isolated forms such as N_S, N-V, and N-V-H. The H3 center is therefore not observed in as-grown CVD synthetic diamond, though it may be introduced by post-growth treatments (Collins, 1978, 1980; Charles et al., 2004; Martineau et al., 2004; Meng et al., 2008).

Creating H3 defects usually involves irradiation and annealing at relatively high temperatures approaching (or including) HPHT conditions. Pre-annealing irradiation introduces vacancies, while annealing mobilizes the necessary nitrogen and vacancy components to form complex nitrogen-aggregated defects, including H3. Modest concentrations of H3 can be formed even without the irradiation step, as long as there is a source of vacancies in the pretreated material (Charles et al., 2004; Martineau et al., 2004; Meng et al., 2008). Annealing temperatures as low as 1500°C have been reported to introduce the H3 defect in CVD synthetic diamond (Meng et al., 2008). H3 in natural diamond is associated with distinct plastic deformation and dislocation features, which release vacancies when annealed either in nature or by laboratory treatment. It is noteworthy, however, that some brown CVD synthetics have low dislocation densities and do not show significant plastic deformation (Martineau et al., 2004; Mäki et al., 2007). Positron annihilation experiments have shown that vacancy clusters can be formed in as-grown CVD synthetic diamond, and that their distribution and size changes after annealing above 1400°C (Mäki et al., 2007).

At typical HPHT-annealing temperatures, N-V and N-V-H defects will break up, N_S may be mobile, and some of the vacancy clusters will dissociate

(Collins, 1980; Charles et al., 2004; Mäki et al., 2007). Thus the formation of H3 in treated CVD synthetic diamond is possible, as the constituents are available and mobile. Significant concentrations of H3 may remain after the treatment so long as the temperature is not sufficiently high to break up the H3 centers.

Analysis of the relative intensities of the H3 (503.2 nm) and N-V centers ($[N\text{-}V]^0$ at 575 nm and $[N\text{-}V]^-$ at 637 nm) may provide information regarding the Gemesis samples' annealing temperature range. A study by Charles et al. (2004) HPHT-annealed different segments of a single CVD synthetic diamond at temperatures of 1900°C (1 hour, 6.5 GPa), 2200°C (1 hour, 7.0 GPa), and 2200°C (10 hours, 7.0 GPa). In PL spectra taken with 488 nm laser excitation, the H3 defect was present after annealing at 1900°C, but less intense than the N-V peaks. Conversely, PL spectra for the CVD sectors annealed at 2200°C displayed a dominant H3 peak. These results agree with those of the HPHT and LPHT (low-pressure, high-temperature) annealing investigation of CVD synthetic diamond by Meng et al. (2008). They found that the N-V peaks were stronger than the H3 peak after LPHT annealing at 1970°C, yet HPHT annealing at 2030°C reversed this relationship. Furthermore, LPHT annealing at 1500°C introduced H3 defects, but their concentration became appreciable only at temperatures above 1700°C. From these published results, it can be inferred that the significant H3 concentrations detected in our Gemesis samples (figure 13) indicated annealing temperatures of at least 1500°C, and probably above 1700°C. The fact that the H3 peaks were less intense than the N-V features suggests that the maximum annealing temperature was ~2000°C.

N3 Center. Another multi-nitrogen defect in diamond, the N3 center (N_3-V) with characteristic emission at 415 nm, has not been observed in as-grown CVD synthetic diamond. Similar to H3, however, this defect can be produced by HPHT-processing a CVD sample, becoming particularly strong after prolonged annealing at 2200°C (Charles et al., 2004; Martineau et al., 2004). This center was weakly detected in 56% of the Gemesis samples.

3123 cm^{-1} Feature. The local vibrational mode at 3123 cm^{-1} is frequently observed in nitrogen-doped CVD synthetics (Wang et al., 2003; Martineau et al., 2004; Khan et al., 2009, 2010). Notably, this absorption was not detected in the Gemesis samples' FTIR spectra. Isotopic substitution experiments using deuterium indicated that the center responsible for the 3123 cm^{-1} line is hydrogen-related (Fuchs et al., 1995a,b; Chevallier et al., 2002). The line has been specifically attributed to $[N\text{-}V\text{-}H]^0$ (Khan et al., 2009, 2010).

The temperature stability of the 3123 cm^{-1} absorption line was investigated by Cruddace (2007) and Cruddace et al. (2007), who annealed CVD-grown diamond samples at temperatures ranging from 900 to 1600ºC, at 100°C increments. The 3123 cm^{-1} line did not start to anneal out until 1200°C, and even then the rate of decay was slow, with ~90% of the initial intensity/concentration remaining after the treatment. Within the uncertainty limits, however, there was no conclusive evidence that the absorption line annealed out until 1500°C. Meng et al. (2008) performed LPHT annealing experiments (1400–2200°C, 150–300 Torr) on single-crystal, as-grown CVD synthetic diamonds in a hydrogen environment using microwave plasma techniques for durations ranging from less than a minute to a few hours. Heating at 1600°C for 10 minutes reduced the intensity of the 3123 cm^{-1} peak (reported as 3124 cm^{-1}), but it was still clearly present. This indicates that even higher temperatures or longer annealing times are needed to entirely anneal out N-V-H centers. The absence of both the 3123 cm^{-1} line in the FTIR spectra and the $[N\text{-}V\text{-}H]^-$ defect in the EPR data (with a detection limit from 5 to 15 ppb) further supports that the Gemesis samples were annealed at temperatures above 1600°C.

3107 cm^{-1} Feature. An IR absorption line at 3107 cm^{-1} is often seen in type I natural diamonds, but only occasionally in type IIa material (Runciman and Carter, 1971; Chrenko et al., 1967; Woods and Collins, 1983; Iakoubovskii and Adriaenssens, 2002). The center responsible for this line can also be introduced into type Ib HPHT-grown synthetics by HPHT annealing at temperatures above 2100°C (Kiflawi et al., 1996). Although not detected in as-grown CVD synthetics, this line has been reported to anneal-in after HPHT treatment at >1700°C (Charles et al., 2004; Martineau et al., 2004; Liggins, 2010; Liggins et al., 2010). While the structure of the defect has not been identified, ^{12}C:^{13}C isotopic substitution experiments have shown that the line originates from a C–H stretch vibration (Woods and Collins, 1983; Kiflawi et al., 1996).

The 3107 cm^{-1} line was not detected in the 16 Gemesis CVD samples. The annealing temperature may not have been high enough to create the center responsible for the feature. Assuming that the reported relationship between the 3107 cm^{-1} line intensity and

nitrogen concentration in HPHT-treated CVD synthetics (Liggins, 2010; Liggins et al., 2010) holds for these lower-nitrogen samples, the resulting concentration of 3107 cm^{-1} centers would be too low to detect.

Synopsis of Evidence for HPHT Treatment. The presence and intensities of H3 and N3, and the absence of $[N\text{-}V\text{-}H]^0$ (3123 cm^{-1}) and $[N\text{-}V\text{-}H]^-$ in the Gemesis samples, strongly suggest annealing temperatures ranging from 1700°C to 2000°C. Although the color saturation of brown diamond decreases after annealing at ~1700°C, it is more likely that temperatures in excess of 1900°C were used to optimize the color change and reduce the necessary annealing time (Meng et al., 2008). However, annealing at these temperatures will lead to graphitization and the destruction of the specimen unless a stabilizing pressure is applied (Davies and Evans, 1972). LPHT annealing (pressure <300 Torr) in the 1400–2200°C range is also possible, though the practice is not widespread (Meng et al., 2008; Liang et al., 2009). Also, the sample must be very carefully prepared prior to LPHT annealing to prevent cracking and graphitization. Thus, it is likely that HPHT treatment was used to improve the color and possibly even the transparency of the Gemesis samples.

The low concentrations of N3, H3, and N-V defects in the Gemesis samples, which were not detected in absorption spectra, suggest that the dominant form of nitrogen impurity is single substitutional nitrogen. Martineau et al. (2004) reported that type IIa (no observable absorption at 1344 cm^{-1}) CVD synthetic diamonds could be grown even when doped with nitrogen. The 1344 cm^{-1} absorption in the majority of the Gemesis samples, and the relatively high N_S^0 concentrations (72 ± 10 to 450 ± 50 ppb), indicate that nitrogen was intentionally introduced during growth. Although nitrogen-doped CVD synthetic diamond is often unappealingly brown (Martineau et al., 2004), the method benefits from significantly higher diamond growth rates (e.g., Tallaire et al., 2005). Hence, it may be commercially viable to produce high-quality colorless or near-colorless CVD products by HPHT treatment of nitrogen-doped brown material.

As-grown faceted CVD synthetics comparable in quality to the Gemesis samples have been produced in the United Kingdom by Element Six Ltd., a De Beers technology company, but these were synthesized purely for research and education purposes (Martineau et al., 2004). They were produced using exhaustive measures to exclude impurities from the growth environment. The technical difficulty, extended growth times, and high cost associated with the synthesis of comparable high-purity as-grown CVD material suggests that manufacturers targeting the colorless diamond sector will instead focus their efforts on developing treatments to improve efficiently produced poor-quality brown material.

Si-Related Defects. Relatively strong doublet emissions at 736.6/736.9 nm (often referred to simply as "737 nm") were recorded in the PL spectra of all the Gemesis CVD samples tested (figure 10A), and this feature was also detected in the UV-Vis-NIR absorption spectra of all but two of the synthetic diamonds in this study (figure 9B).

The detection of silicon impurities in diamond is usually verified by the 737 nm line in either PL or absorption spectra (Clark et al., 1995). Natural type Ia and type IIa diamonds rarely show this feature, which was first reported in natural specimens by Breeding and Wang (2008). Since then it has been observed in several natural stones, but far less than 1% of those studied by GIA (unpublished data). Conversely, silicon is often unintentionally introduced into CVD synthetic diamond by the etching of Si-containing components in the reactor, such as silica windows (Robins et al., 1989; Barjon et al., 2005). Although the feature is not specific to CVD, it has often been part of gemological identification criteria (Wang et al., 2003, 2007; Martineau et al., 2004). Si-V centers have high temperature stability, withstanding annealing up to 2200°C (Clark and Dickerson, 1991). Therefore, it is not surprising that the Gemesis CVD samples contain this defect. A line at 946 nm, observed in Si-containing diamond in both absorption and emission, has been attributed to $[Si\text{-}V]^0$ (Evans et al., 2006; D'Haenens-Johansson et al., 2010, 2011). The 946 nm peak was not observed in the absorption spectra of the Gemesis samples. Since the 737 nm peak intensity revealed by absorption spectroscopy was weak (e.g., figure 9B) it would not be surprising if the 946 nm peak was below the detection limit. PL spectroscopy (830.0 nm excitation), which has a higher sensitivity than absorption spectroscopy, detected the 946 nm peak in five samples (GS03, GS08, GS10, GS13, and GS14).

Identification Features. Separating these new CVD synthetic diamonds from their natural counterparts is becoming increasingly difficult using conventional gemological procedures, and may not even be possible without advanced spectroscopic techniques. The color and clarity grades, as well as weak interference colors and birefringence patterns, are comparable to those

seen in natural diamonds. The H3 defect is common in natural type IIa diamonds, and the associated green fluorescence is frequently observed. Small black irregular inclusions such as those seen in CVD synthetic diamond are occasionally observed in natural stones. However, the petal-shaped, highly localized stress patterns around such inclusions are good indicators of CVD synthesis.

Previous studies relied heavily on infrared absorption spectroscopy for the identification of CVD synthetic diamonds, citing features such as the absorption line at 3123 cm^{-1}. With further developments in growth techniques and post-growth treatment, however, infrared absorption spectroscopy of the samples in this study did not show identification features that easily separated them from natural or HPHT-grown synthetic type IIa diamonds. Instead, our samples displayed mid- and near-IR spectra that were remarkably similar to those of natural type IIa diamond. Traces of isolated nitrogen in a type IIa sample have generally served as an alert to CVD growth, but N_S^0 was hardly detectable in these specimens—and HPHT-treated natural type IIa diamonds can also contain isolated nitrogen.

The most useful identification features were revealed by PL spectroscopy and DiamondView fluorescence images. Strong emissions of $[Si\text{-}V]^-$ at 736.6 and 736.9 nm were observed in all of the samples, and this defect was also detected in the UV-Vis-NIR spectra of most samples. Its presence remains a very strong (but not conclusive) indication of CVD synthesis. Very few natural type IIa diamonds show these emissions (Breeding and Wang, 2008). Emission at 946 nm from the $[Si\text{-}V]^0$ optical center was detected in one-third of the samples. Because this feature has not been reported in natural diamond, it can be used to indicate CVD synthesis. In the DiamondView, fine growth striations are a unique feature of CVD synthetic diamond. While the point defects (including $[Si\text{-}V]^-$) can be removed or modified by post-growth treatment, the growth striations remain unchanged. For example, H-related absorption in the infrared region was destroyed and the H3 center was introduced in the samples we studied, but the striations were still clearly observable. The distribution of H3 centers actually followed the striations, as shown by the DiamondView images in figure 4. Another interesting feature was the series of sharp emission peaks in the 495–580 nm region revealed by 488.0 and 514.5 nm laser excitations, such as those at 525.4, 535.1, 540.4, 546.1, and 572.9 nm (figures 10B and 13). While their assignment is unclear, their occurrence as a group could offer a reliable indication of CVD growth.

In short, CVD synthetic diamonds from Gemesis are entirely identifiable. Proper analysis using PL spectroscopy and fluorescence imaging techniques is critical to ensuring that these materials are clearly distinguished from their type IIa counterparts, such as natural, natural but HPHT treated, and HPHT-grown synthetic diamonds.

CONCLUDING REMARKS

The new CVD synthetic diamonds from Gemesis showed clear improvements over those reported previously from other sources. These gems average nearly half a carat, the most popular diamond weight in the marketplace, and their color and clarity are comparable to top-quality natural diamonds. These synthetic materials can be identified with a combination of photoluminescence and UV fluorescence imaging techniques. There is no question that the size and quality of CVD synthetic diamonds will continue improving. Post-growth treatment improves color and possibly clarity. It appears that the striated growth pattern of CVD synthetic diamonds cannot be altered by any treatment, so it remains the most important if not the only visual identification feature.

ABOUT THE AUTHORS

Dr. Wang (wwang@gia.edu) is the director of research and development, Dr. D'Haenens-Johansson is a research scientist, Mr. Johnson is the supervisor of diamond advanced testing, Mr. Moe is a research associate, and Mr. Moses is senior vice president at GIA's New York laboratory. Ms. Emerson was a research technician at GIA and is currently working on her master's degree. Dr. Newton is a professor in experimental physics at the University of Warwick, UK.

ACKNOWLEDGMENTS

The authors thank Ivana Kayes, Siau Fung Yeung, and Dr. Christopher M. Breeding of GIA's New York and Carlsbad laboratories for their many suggestions and assistance with this study. Dr. Christopher Welbourn at the University of Warwick is thanked for his help with EPR analysis. We are grateful to Stephen Lux of Gemesis Corp. for providing the samples for this study.

REFERENCES

Avalos V., Dannefaer S. (2003) Vacancy-type defects in brown diamonds investigated by positron annihilation. *Physica B*, Vol. 340–342, pp. 76–79, http://dx.doi.org/10.1016/j.physb.2003.09.006.

Bangert U., Barnes R., Gass M.H., Bleloch A.L., Godfrey I.S. (2009) Vacancy clusters, dislocations and brown colouration in diamond. *Journal of Physics: Condensed Matter*, Vol. 21, No. 36, article 364208, http://dx.doi.org/10.1088/0953-8984/21/36/364208.

Barjon J., Rzepka E., Jomard F., Laroche J.-M., Ballutaud D., Kociniewski T., Chevallier J. (2005) Silicon incorporation in CVD diamond layers. *Physica Status Solidi* (a), Vol. 202, No. 11, pp. 2177–2181, http://dx.doi.org/10.1002/pssa.200561920.

Breeding C.M., Wang W. (2008) Occurrence of the Si-V defect in natural colorless gem diamonds. *Diamond and Related Materials*, Vol. 17, No. 7–10, pp. 1335–1344, http://dx.doi.org/10.1016/j.diamond.2008.01.075.

Butler J.E., Mankelevich Y.A., Cheesman A., Ma J., Ashfold M.N.R. (2009) Understanding the chemical vapor deposition of diamond: Recent progress. *Journal of Physics: Condensed Matter*, Vol. 21, article 364201, http://dx.doi.org/ 10.1088/0953-8984/21/36/364201.

Chadwick K. (2008a) Lab Notes: First CVD synthetic diamond submitted for Dossier grading. *G&G*, Vol. 44, No. 1, pp. 67–69.

Chadwick K. (2008b) Lab Notes: HPHT-treated CVD synthetic diamond submitted for Dossier grading. *G&G*, Vol. 44, No. 4, pp. 365–367.

Charles S.J., Butler J.E., Feygelson B.N., Newton M.E., Carroll D.L., Steeds J.W., Darwish H., Yan C.-S., Mao H.K., Hemley R.J. (2004) Characterization of nitrogen doped chemical vapor deposited single crystal diamond before and after high pressure, high temperature annealing. *Physica Status Solidi (a)*, Vol. 201, No. 11, pp. 2473–2485, http://dx.doi.org/10.1002/pssa.200405175.

Chevallier J., Jomard F., Teukam Z., Koizumi S., Kanda H., Sato Y., Deneuville A., Bernard M. (2002) Hydrogen in n-type diamond. *Diamond and Related Materials*, Vol. 11, pp. 1566–1571, http://dx.doi.org/10.1016/S0925-9635(02)00063-8.

Chrenko R.M., McDonald R.S., Barrow K.A. (1967) Infra-red spectra of diamond coat. *Nature*, Vol. 213, pp. 474–476, http://dx.doi.org/10.1038/213474a0.

Clark C.D, Dickerson C.B. (1991) The 1.681 eV center in polycrystalline diamond. *Surface and Coatings Technology*, Vol. 47, No. 1–3, pp. 336–343, http://dx.doi.org/10.1016/0257-8972(91)90299-C.

Clark C.D., Kanda H., Kiflawi I., Sittas G. (1995) Silicon defects in diamond. *Physical Review B*, Vol. 51, No. 23, pp. 16681–16688, http://dx.doi.org/10.1103/PhysRevB.51.16681.

Collins A.T. (1978) Migration of nitrogen in electron-irradiated type Ib diamond. *Journal of Physics C: Solid State Physics*, Vol. 11, No. 10, pp. L417–L422, http://dx.doi.org/10.1088/0022-3719/11/10/002.

——— (1980) Vacancy enhanced aggregation of nitrogen in diamond. *Journal of Physics C: Solid State Physics*, Vol. 13, No. 14, pp. 2641–2650, http://dx.doi.org/10.1088/0022-3719/13/14/006.

Collins A.T., Stanley M., Woods G.S. (1987) Nitrogen isotope effects in synthetic diamonds. *Journal of Physics D: Applied Physics*, Vol. 20, No. 7, pp. 969–974, http://dx.doi.org/10.1088/0022-3727/20/7/022.

Collins A.T., Kanda H., Kitawaki H. (2000) Colour changes produced in natural brown diamonds by high-pressure, high-temperature treatment. *Diamond and Related Materials*, Vol. 9, No. 2, pp. 113–122, http://dx.doi.org/10.1016/S0925-9635(00)00249-1.

Cox A., Newton M.E., Baker J.M. (1994) ^{13}C, ^{14}N and ^{15}N ENDOR measurements on the single substitutional nitrogen centre (P1) in diamond. *Journal of Physics: Condensed Matter*, Vol. 6, No. 2, pp. 551–563, http://dx.doi.org/10.1088/0953-8984/6/2/025.

Cruddace R.C. (2007) Magnetic Resonance and Optical Studies of Point Defects in Single Crystal CVD Diamond. Ph.D. Thesis, University of Warwick, UK.

Cruddace R.C., Newton M.E., Smith H.E., Davies G., Martineau P.M., Twitchen D.J. (2007) Identification of the 3123 cm^{-1} absorption line in SC-CVD diamond as the NVH^- defect. *Proceedings of the 58th De Beers Diamond Conference*, Coventry, UK, July 11–13, Poster No. 15.

Davies G. (1974) Vibronic spectra in diamond. *Journal of Physics C: Solid State Physics*, Vol. 7, No. 20, pp. 3797–3809, http://dx.doi.org/10.1088/0022-3719/7/20/019.

Davies G., Evans T. (1972) Graphitization of diamond at zero pressure and at high pressure. *Proceedings of the Royal Society of London A*, Vol. 328, No. 1574, pp. 413–427, http://dx.doi.org/10.1098/rspa.1972.0086.

Davies G., Welbourn C.M., Loubser J.H.N. (1978) Optical and electron paramagnetic effects in yellow type Ia diamonds. *Diamond Research*, pp. 23–30.

D'Haenens-Johansson U.F.S., Edmonds A.M., Newton M.E., Goss J.P., Briddon P.R., Baker J.M., Martineau P.M., Khan R.U.A., Twitchen D.J., Williams S.D. (2010) EPR of a defect in CVD diamond involving both silicon and hydrogen that shows preferential alignment. *Physical Review B*, Vol. 82, No. 15, article 155205, http://dx.doi.org/10.1103/PhysRevB.82.155205.

D'Haenens-Johansson U.F.S., Edmonds A.M., Green B.L., Newton M.E., Davies G., Martineau P.M., Khan R.U.A., Twitchen D.J. (2011) Optical properties of the neutral silicon split-vacancy center in diamond. *Physical Review B*, Vol. 84, No. 24, article 245208, http://dx.doi.org/10.1103/PhysRevB.84.245208.

Doering P.J., Linares R.C. (1999) Large area single crystal CVD diamond: Properties and applications. *Proceedings of Applied Diamond Conference/Frontier Carbon Technology Joint Conference 1999*, Tsukuba, Japan, Aug. 31–Sept. 3, pp. 32–35.

Dyer H.B., Raal F.A., Du Preez L., Loubser J.H.N. (1965) Optical absorption features associated with paramagnetic nitrogen in diamond. *Philosophical Magazine*, Vol. 11, No. 112, pp. 763–774, http://dx.doi.org/10.1080/14786436508230081.

Edmonds A.M., Newton M.E., Martineau P.M., Twitchen D.J., Williams S.D. (2008) Electron paramagnetic resonance studies of silicon-related defects in diamond. *Physical Review*, Vol. 77, No. 24, article 245205, http://dx.doi.org/10.1103/PhysRevB.77.245205.

Evans D.J.F., Kelly C.J., Leno P., Martineau P.M., Taylor A.J. (2006) Silicon doped single crystal CVD diamond grown using silane. *Proceedings of the 57th De Beers Diamond Conference*, Cambridge, UK, July 10–12, pp. 38–40.

Fall C.J., Blumenau A.T., Jones R., Briddon P.R., Frauenheim T., Gutierrez-Sosa A., Bangert U., Mora A.E., Steeds J.W., Butler J.E. (2002) Dislocations in diamond: Electron energy-loss spectroscopy. *Physical Review B*, Vol. 65, No. 20, article 205206, http://dx.doi.org/10.1103/PhysRevB.65.205206.

Fisher D., Spits R.A. (2000) Spectroscopic evidence of GE POL HPHT-treated natural type IIa diamonds. *G&G*, Vol. 36, No. 1, pp. 42–49, http://dx.doi.org/10.5741/GEMS.36.1.42.

Fisher D., Evans D.J.F., Glover C., Kelly C.J., Sheehy M.J., Summerton G.C. (2006) The vacancy as a probe of the strain in type IIa diamonds. *Diamond and Related Materials*, Vol. 15, No. 10, pp. 1636–1642, http://dx.doi.org/10.1016/j.diamond.2006.01.020.

Fisher D., Sibley S.J., Kelly C.J. (2009) Brown colour in natural diamond and interaction between the brown related and other colour-inducing defects. *Journal of Physics: Condensed Matter*, Vol. 21, No. 36, article 364213, http://dx.doi.org/10.1088/0953-8984/21/36/364213.

Fuchs F., Wild C., Schwarz K., Koidl P. (1995a) Hydrogen-related IR absorption in chemical vapour deposited diamond. *Diamond and Related Materials*, Vol. 4, No. 5–6, pp. 652–656, http://dx.doi.org/10.1016/0925-9635(94)05247-6.

Fuchs F., Wild C., Schwarz K., Muller-Sebert W., Koidl P. (1995b) Hydrogen induced vibrational and electronic transitions in chemical vapor deposited diamond, identified by isotopic sub-

stitution. *Applied Physics Letters*, Vol. 66, No. 2, pp. 177–179, http://dx.doi.org/10.1063/1.113126.
Glover C., Newton M.E., Martineau P., Twitchen D.J., Baker J.M. (2003) Hydrogen incorporation in diamond: The nitrogen-vacancy-hydrogen complex. *Physical Review Letters*, Vol. 90, No. 18, article 185507, http://dx.doi.org/10.1103/PhysRevLett.90.185507.
Glover C., Newton M.E., Martineau P.M., Quinn S., Twitchen D.J. (2004) Hydrogen incorporation in diamond: The vacancy-hydrogen complex. *Physical Review Letters*, Vol. 92, No. 13, article 135502, tp://dx.doi.org/10.1103/PhysRevLett.92.135502.
Goodwin D.G., Butler J.E. (1997) Theory of diamond chemical vapor deposition. In M.A. Prelas, G. Popovici, and L.K. Biglow, Eds., *Handbook of Industrial Diamonds and Diamond Films*, Marcel Dekker Inc., New York, pp. 527–581.
Goss J.P., Jones R., Breuer S.J., Briddon P.R., Oberg S. (1996) The twelve-line 1.682 eV luminescence center in diamond and the vacancy-silicon complex. *Physical Review Letters*, Vol. 77, No. 14, pp. 3041–3044, http://dx.doi.org/10.1103/PhysRevLett.77.3041.
Graff M. (2010) Gemesis to sell lab-grown whites to consumers. *National Jeweler*, http://www.nationaljeweler.com/nj/diamonds/a/~20714-Gemesis-to-sell-labgrown-whites [date accessed: May 14, 2012].
Hounsome L.S., Jones R., Martineau P.M., Fisher D., Shaw M.J., Briddon P.R., Öberg S. (2006) Origin of brown coloration in diamond. *Physical Review B*, Vol. 73, No. 12, article 125203, http://dx.doi.org/10.1103/PhysRevB.73.125203.
Iakoubovskii K., Adriaenssens G.J. (2002) Optical characterization of natural Argyle diamonds. *Diamond and Related Materials*, Vol. 11, No. 1, pp. 125–131, http://dx.doi.org/10.1016/S0925-9635(01)00533-7.
Khan R.U.A., Martineau P.M., Cann B.L., Newton M.E., Twitchen D.J. (2009) Charge transfer effects, thermo and photochromism in single crystal CVD synthetic diamond. *Journal of Physics: Condensed Matter*, Vol. 21, No. 36, article 364214, http://dx.doi.org/10.1088/0953-8984/21/36/364214.
Khan R.U.A., Martineau P.M., Cann B.L., Newton M.E., Dhillon H.K., Twitchen D.J. (2010) Color alterations in CVD synthetic diamond with heat and UV exposure: Implications for color grading and identification. *G&G*, Vol. 18, No. 2, pp. 18–26, http://dx.doi.org/10.5741/GEMS.18.2.18.
Kiflawi I., Mainwood A., Kanda H., Fisher D. (1996) Nitrogen interstitials in diamond. *Physical Review B*, Vol. 54, No. 23, pp. 16719–16726, http://dx.doi.org/10.1103/PhysRevB.54.16719.
Lawson S.C., Fisher D., Hunt D.C., Newton M.E. (1998) On the existence of positively charged single-substitutional nitrogen in diamond. *Journal of Physics: Condensed Matter*, Vol. 10, No. 27, pp. 6171–6180, http://dx.doi.org/10.1088/0953-8984/10/27/016.
Liang Q, Yan C.-S., Meng Y., Lai J., Krasnicki S., Mao H.-K., Hemley R.J. (2009) Recent advances in high-growth rate single-crystal CVD diamond. *Diamond and Related Materials*, Vol. 18, pp. 698–703, http://dx.doi.org/10.1016/j.diamond.2008.12.002.
Liggins S. (2010) Identification of Point Defects in Treated Single Crystal Diamond. Ph.D. thesis, University of Warwick, UK.
Liggins S., Cruddace R.J., Cann B.L., Newton M.E., Khan R.U.A., Martineau P.M., Twitchen D.J., Goss J.P., Briddon P.R. (2010) Studies of hydrogen related defects in diamond. *61st De Beers Diamond Conference*, University of Warwick, Coventry, UK, July 11–13, Poster No. 23.
Linares R.C., Doering P.J. (1999) Properties of large single crystal diamond. *Diamond and Related Materials*, Vol. 8, No. 2–5, pp. 909–915, http://dx.doi.org/10.1016/S0925-9635(98)00382-3.
Mäki J.-M., Tuomisto F., Kelly C., Fisher D., Martineau P. (2007) Effects of thermal treatment on optically active vacancy defects in CVD diamonds. *Physica B*, Vol. 401–402, pp. 613–616, http://dx.doi.org/10.1016/j.physb.2007.09.034.
Martineau P.M., Lawson S.C., Taylor A.J., Quinn S.J., Evans D.J.F., Crowder M.J. (2004) Identification of synthetic diamond grown using chemical vapor deposition (CVD). *G&G*, Vol. 40, No. 1, pp. 2–25, http://dx.doi.org/10.5741/GEMS.40.1.2.
Martineau P.M., Gaukroger M., Khan R., Evans D. (2009) Effect of steps on dislocations in CVD diamond grown on {001} substrates. *Physica Status Solidi C*, Vol. 6, No. 8, pp. 1953–1957, http://dx.doi.org/10.1002/pssc.200881465.
Meng Y.F., Yan C.S., Lai J., Krasnicki S., Shu H., Yu T., Ling Q., Mao H.K., Hemley R.J. (2008) Enhanced optical properties of chemical vapor deposited single crystal diamond by low-pressure/high-temperature annealing. *Proceedings of the National Academy of Sciences*, Vol. 105, No. 46, pp. 17620–17625, http://dx.doi.org/10.1073/pnas.0808230105.
Moses T.M., Shigley J.E., McClure S.F., Koivula J.I., Van Daele M. (1999) Observations on GE-processes diamonds: A photographic record. *G&G*, Vol. 35, No. 3, pp. 14–22, http://dx.doi.org/10.5741/GEMS.35.3.14.
Robins L.H., Cook L.P., Farabaugh E.N., Feldman A. (1989) Cathodoluminescence of defects in diamond films and particles grown by hot-filament chemical-vapor deposition. *Physical Review B*, Vol. 39, No. 18, pp. 13367–13377, http:// dx.doi.org//10.1103/PhysRevB.39.13367.
Runciman W.A., Carter T. (1971) High resolution infra-red spectra of diamond. *Solid State Communications*, Vol. 9, No. 5, pp. 315–317, http://dx.doi.org/10.1016/0038-1098(71)90001-9.
Smith W., Sorokin P.P., Gelles I.L., Lasher G.J. (1959) Electron-spin resonance of nitrogen donors in diamond. *Physical Review*, Vol. 115, No. 6, pp. 1546–1552, http://dx.doi.org/10.1103/PhysRev.115.1546.
Tallaire A., Achard J., Sussmann R.S., Silva F., Gicquel A. (2005) Homoepitaxial deposition of high-quality thick diamond films: Effect of growth parameters. *Diamond and Related Materials*, Vol. 14, No. 3–7, pp. 249–254, http://dx.doi.org/10.1016/j.diamond.2004.10.037.
Vavilov V.S., Gippius A.A., Zaitsev B.V., Deryagin B.V., Spitsyn B.V., Aleksenko A.E. (1980) Investigation of the cathodoluminescence of epitaxial diamond films. *Soviet Physics-Semiconductors*, Vol. 14, pp. 1078–1079.
Wang W., Moses T.M. (2011) Lab Notes: Gem-quality CVD synthetic diamonds from Gemesis. *G&G*, Vol. 47, No. 3, pp. 227–228.
Wang W., Moses T., Linares R., Shigley J.E., Hall M., Butler J.E. (2003) Gem-quality synthetic diamonds grown by the chemical vapor deposition method. *G&G*, Vol. 39, No. 4, pp. 268–283, http://dx.doi.org/10.5741/GEMS.39.4.268.
Wang W., Tallaire A., Hall M.S., Moses T.M., Achard J., Sussmann R.S., Gicquel A. (2005) Experimental CVD synthetic diamonds from LIMHP-CNRS, France. *G&G*, Vol. 41, No. 3, pp. 234–244, http://dx.doi.org/10.5741/GEMS.41.3.234.
Wang W., Hall M.S., Moe K.S., Tower J., Moses T.M. (2007) Latest-generation CVD-grown synthetic diamonds from Apollo Diamond Inc. *G&G*, Vol. 43, No. 4, pp. 294–312, http://dx.doi.org/10.5741/GEMS.43.4.294.
Wang W., Doering P., Tower J., Lu R., Eaton-Magana S., Johnson P., Emerson E., Moses T.M. (2010) Strongly colored pink CVD lab-grown diamonds. *G&G*, Vol. 46, No. 1, pp. 4–17, http://dx.doi.org/10.5741/GEMS.46.1.4.
Welbourn C.M., Cooper M., Spear P.M. (1996) De Beers natural versus synthetic diamond verification instruments. *G&G*, Vol. 32, No. 3, pp. 156–169, http://dx.doi.org/10.5741/GEMS.32.3.156.
Willems B., Martineau P.M., Fisher D., Van Royen J., Van Tendeloo G. (2006) Dislocation distributions in brown diamond. *Physica Status Solidi (a)*, Vol. 203, pp. 3076–3080, http://dx.doi.org/10.1002/pssa.200671129.
Woods G.S., Collins A.T. (1983) Infrared absorption spectra of hydrogen complexes in type I diamonds. *Journal of Physics and Chemistry of Solids*, Vol. 44, No. 5, pp. 471–475, http://dx.doi.org/10.1016/0022-3697(83)90078-1.